Comput Geosci (2007) 11:73–85
DOI 10.1007/s10596-006-9035-5

ORIGINAL PAPER

Application of the representer method for parameter estimation in numerical reservoir models

Justyna K. Przybysz-Jarnut · Remus G. Hanea · Jan-Dirk Jansen · Arnold W. Heemink

Received: 23 May 2005 / Accepted: 20 November 2006 / Published online: 21 December 2006

Abstract A data assimilation method was applied to estimate poorly known parameters (permeabilities) in a numerical reservoir model. Most variational methods for data assimilation are based on the assumption that the model is perfect except for the poorly known parameters. The representer method allows also for model errors, i.e. for uncertainties in the state variables (pressures and saturations). The method is based on minimizing a cost functional, assuming all the errors and parameters to be multivariate Gaussian random variables with given mean and covariances. The uncertain parameters and variables are expanded into a finite sum of basis functions called representers, and the gradients of the cost functional are obtained with an adjoint method. This approach gives an optimal parametrization in the sense that the final result is equal to the solution of the full inverse problem. The method was tested on a simple one-dimensional model to simulate two-phase (oil-water) flow through a heterogeneous reservoir. The results show that the method is able to provide an acceptable estimate of the permeability field. We used pressure measurements from a small number of observation wells in between the injection and production wells, but the representer method could be used equally well to assimilate data from other sources. The method appears to be a promising data assimilation tool for applications in reservoir engineering.

Keywords adjoint method · automatic history matching · Euler–Lagrange equations · one-dimensional two-phase flow · representer method

J. K. Przybysz-Jarnut (✉)
Laboratory of Acoustical Imaging and Sound Control,
Lorentzweg 1, P.O. Box 5046, 2600 GA Delft,
2628 CJ Delft, The Netherlands
e-mail: justyna@akst.tn.tudelft.nl

J. K. Przybysz-Jarnut
Faculty of Applied Physics,
Department of Imaging Science and Technology,
Delft University of Technology, Delft, The Netherlands

R. G. Hanea · A. W. Heemink
Faculty of Electrical Engineering,
Mathematics and Computer Science,
Delft Institute of Applied Mathematics,
Delft University of Technology, Delft, The Netherlands

J.-D. Jansen
Faculty of Civil Engineering and Geosciences,
Department of Geotechnology,
Delft University of Technology, Delft, The Netherlands

1 Introduction

The properties of reservoir rocks have an important influence on the hydrocarbon recovery process. These are not known in detail for the whole reservoir, but only for the neighborhood of the wells. The numerical values for those properties are obtained from measurements resulting from imperfect measuring techniques. Furthermore, there are also uncertainties in the fluid properties and the amount of hydrocarbons present in the reservoir. All those circumstances influence the effectiveness of techniques used to drain the reservoir. During the past decades, several "automatic history matching" techniques have been developed to

adapt the parameters of a numerical reservoir model using pressures and flow rates as measured during the production process [5, 6, 9]. These techniques are somewhat similar to data assimilation methods as applied in, for example, oceanography and meteorology [2, 3], atmospheric chemistry and transport modelling [15], and groundwater flow [14]. In data assimilation, all the information present in measurements from various sources is combined with the information obtained from the evaluation of a dynamical model with the aim to produce better forecasts. There are two kinds of data assimilation methods: the sequential approach involving Kalman filtering [8] or particle filters, and the non-sequential approach involving variational adjoint-based methods [13].

In the adjoint method, the model is usually considered to be perfect, and the uncertainties are due to uncertain parameters. The method focuses on estimating uncertain parameters while keeping all the error terms as small as possible. The representer method [2] allows for inclusion of the uncertainties both in the model and parameters. The best fit to all data is defined in the least-squares sense. The method was originally designed for linear models, but it has later also been used for nonlinear dynamics, yielding satisfactory results [4, 14].

The representer algorithm assumes linearity of the dynamics and observing systems [3]. It allows for estimation of both the state variables and the parameters. Unfortunately, inclusion of parameter estimation makes the problem nonlinear, even for linear dynamics. Iterative solution schemes have been developed, but the convergence of those schemes is not guaranteed [4, 14]. For strongly nonlinear dynamics, parameter estimation is extremely difficult, especially if many parameters are estimated at the same time.

The reservoir model used in this study is described in Section 2. Section 3 presents the derivation of the representer method for the underlying flow model. The results of the data assimilation calculations for a twin experiment are presented and discussed in Section 4. The conclusions are given in Section 5.

2 Formulation of the forward model

Consider a one-dimensional immiscible two-phase (oil–water) injection–production situation in a porous conduit with unit cross-sectional area. The boundary of the domain Ω is divided according to Dirichlet and Neumann boundary conditions, Γ_D and Γ_N, respectively. The system is described by a set of two partial differential equations, one for pressure and one for saturation, together with initial and boundary conditions.

The pressure equation is given by:

$$\phi c \frac{\partial p}{\partial t} - \frac{\partial}{\partial x}\lambda \frac{\partial p}{\partial x} = 0 \qquad \text{on } \Omega \times (0, T] \tag{1}$$

$$p = P_I \qquad \text{on } \Omega \times \{0\} \tag{2}$$

$$\frac{\partial p}{\partial x} = P_N \qquad \text{on } \Gamma_N \times (0, T] \tag{3}$$

$$p = P_D \qquad \text{on } \Gamma_D \times (0, T], \tag{4}$$

where p denotes oil pressure (which is, in our case, identical to water pressure), ϕ denotes porosity, and c denotes total compressibility and is regarded here as a function of constant rock, oil and water compressibilities, and water saturation S:

$$c(S) = c_r + Sc_w + (1 - S)c_o. \tag{5}$$

λ is the total mobility and it is a function of water saturation and absolute permeability k:

$$\lambda(S, k) = \lambda_w(S, k) + \lambda_o(S, k) = \frac{kk_{rw}(S)}{\mu_w} + \frac{kk_{ro}(S)}{\mu_o}, \tag{6}$$

where k_{rw} and k_{ro} are the water and oil relative permeabilities, respectively, and μ_w and μ_o are constant water and oil viscosities, respectively.

The saturation equation is given by:

$$D\frac{\partial^2 S}{\partial x^2} - v\frac{\partial S}{\partial x} - \phi\frac{\partial S}{\partial t} = 0 \qquad \text{on } \Omega \times (0, T] \tag{7}$$

$$S = S_I \qquad \text{on } \Omega \times \{0\} \tag{8}$$

$$\frac{\partial S}{\partial x} = S_N \qquad \text{on } \Gamma_N \times (0, T] \tag{9}$$

$$S = S_D \qquad \text{on } \Gamma_D \times (0, T], \tag{10}$$

where S denotes water saturation, D is a constant diffusion coefficient, and v is total velocity as a function of pressure, saturation, and permeability:

$$v(p, S, k) = -\lambda_w\frac{\partial p}{\partial x} - \lambda_o\frac{\partial p}{\partial x}. \tag{11}$$

The absolute permeability is assumed to vary only in space.

Because some parameters are functions of either pressure or saturation, the systems 1–4 and 7–10 are coupled.

2.1 Discretized forward model

The reservoir model is usually solved using numerical models based on a finite difference discretization schemes [1, 10]. Here the implicit pressure-explicit saturation method was adapted. The discretized system can be written in matrix form as [11]:

$$\mathbf{A}(S_{j-1}, k)\mathbf{p}_j = \mathbf{B}(S_{j-1})\mathbf{p}_{j-1} + \mathbf{d}(S_{j-1}, k); \quad j = 1, ..., M \tag{12}$$

$$\mathbf{p}_0 = \mathbf{p}_{\text{init}} \tag{13}$$

$$\mathbf{S}_j = \mathbf{F}(S_{j-1}, p_j, k)\mathbf{S}_{j-1} + \mathbf{g}(S_{j-1}, p_j, k) \tag{14}$$

$$\mathbf{S}_0 = \mathbf{S}_{\text{init}}, \tag{15}$$

where **A**, **B**, and **F** are coefficient matrices that depend on either permeability, pressure, or saturation (shown by the brackets following a matrix), **d** and **g** are vectors of corresponding forcing terms that depend on the boundary conditions, **p** and **S** are vectors of pressure and saturation, $\mathbf{p}_{\text{init}}$ and $\mathbf{S}_{\text{init}}$ are the initial conditions for pressure and saturation and M denotes the number of time steps.

3 Inverse problem

Suppose that the additional information is given by a set of discrete measurements taken at isolated points in space and time, and related to observable variables by:

$$\mathbf{z} = M(p) + \boldsymbol{\nu}, \tag{16}$$

where **z** is a vector of all measurements and $\boldsymbol{\nu}$ is a vector of random measurement errors. The measurement operator $M(\cdot)$ describes how a particular measurement is related to the pressure. In this study, all measurements are represented by pressure measurements so the operator $M(\cdot)$ is linear and is replaced in the following sections by p_{mes} or measured pressure.

With the measurements available, the problem becomes over-determined, and the goal is to find a solution that corresponds to the smallest errors in the least-squares sense.

To account for model errors caused by imperfectly modelled inputs and various simplifying assumptions, the error terms are introduced in the reservoir model. They act as additional forcing terms and depend on time for both the pressure and saturation equation. The true pressures and saturations obey the following stochastic state equations:

$$\mathbf{A}(S_{j-1}, k)\mathbf{p}_j = \mathbf{B}(S_{j-1})\mathbf{p}_{j-1} + \mathbf{d}(S_{j-1}, k) + \boldsymbol{\epsilon}_j; \quad j = 1, ..., M \tag{17}$$

$$\mathbf{p}_0 = \mathbf{p}_{\text{init}} \tag{18}$$

$$\mathbf{S}_j = \mathbf{F}(S_{j-1}, p_j, k)\mathbf{S}_{j-1} + \mathbf{g}(S_{j-1}, p_j, k) + \mathbf{w}_j \tag{19}$$

$$\mathbf{S}_0 = \mathbf{S}_{\text{init}}, \tag{20}$$

where $\boldsymbol{\epsilon}_j$ and $\mathbf{w}_j$ are the pressure and saturation model errors, respectively.

The next step is to combine the information that comes from measurements with that given by a forward model to produce the best fit to all the information in a least-squares sense [3]. Therefore, we need an optimal estimate that minimizes the following objective function:

$$J = (\mathbf{z} - \mathbf{p}_{\text{mes}})^T \mathbf{P}_v^{-1} (\mathbf{z} - \mathbf{p}_{\text{mes}}) + (\mathbf{k} - \bar{\mathbf{k}})^T \mathbf{P}_k^{-1} (\mathbf{k} - \bar{\mathbf{k}}) + \sum_{j=1}^{M} \boldsymbol{\epsilon}_j^T \mathbf{P}_{\epsilon_j}^{-1} \boldsymbol{\epsilon}_j + \sum_{j=1}^{M} \mathbf{w}_j^T \mathbf{P}_{w_j}^{-1} \mathbf{w}_j, \tag{21}$$

where **k** represents the vector of permeabilities at the grid points and $\bar{\mathbf{k}}$ is the prior estimate of these parameters. $\mathbf{P}_v^{-1}$, $\mathbf{P}_k^{-1}$, $\mathbf{P}_{\epsilon_j}^{-1}$, and $\mathbf{P}_{w_j}^{-1}$ are weighting matrices and reflect our belief in the observation model, the prior estimate for the parameters, and the dynamical model, respectively. The least-squares approach has no probabilistic meaning [8]. If the parameters and error terms are considered random variables, the solution to the inverse problem is found by determining the joint posterior probability density function of parameters, model, and measurement errors, given the measurements [14]. This represents the maximum a posteriori estimate. In general, it is not straightforward to find the maximum of this probability density function. However, in the particular case where all the model errors, parameters, and measurement errors are Gaussian- distributed with known mean and covariance and not cross-correlated, the maximum a posteriori estimate is the mode of this posterior probability density function [12]. Finding the maximum of this posterior density is equivalent with minimizing the objective function given in (21) with the weighting matrices replaced by the respective covariance matrices. In this case, model errors are normally distributed with mean zero and covariances $\mathbf{P}_{\epsilon_j}$, $\mathbf{P}_{w_j}$, measurement errors with mean zero and covariance $\mathbf{P}_v$, and parameters with mean $\bar{\mathbf{k}}$ and covariance matrix $\mathbf{P}_k$.

This penalty functional consists of four terms. The first term represents the discrepancies between observations and the model predictions for those observations, the second term ensures that the estimate of parameters will stay close to the prior mean, and the third and fourth terms penalize the model errors. The optimal estimates are obtained when the sum of those four terms is minimal.

3.1 Euler–Lagrange conditions

The minimum of the given penalty functional must be found under the constraint that the forward model is satisfied within error bounds. To accomplish this restriction, the penalty functional is augmented by inclusion of model equations multiplied by Lagrange multipliers **L**. Based on the theory of calculus and variations [7], the local minimum is found if the first variation of a penalty function with respect to state variables, Lagrange multipliers, parameters, and model errors vanishes. This condition leads to the system of Euler–Lagrange equations, which consists of two adjoint systems, the parameter equation, and two forward systems (a short derivation is given in Appendix B):

$$\mathbf{A}^{\mathrm{T}}\mathbf{L}_{jp} = \mathbf{B}^{\mathrm{T}}\mathbf{L}_{(j+1)p} + \left[\frac{\partial\left[\mathbf{F}\mathbf{S}_{j-1}\right]^{\mathrm{T}}}{\partial \mathbf{p}_j} + \frac{\partial \mathbf{g}^{\mathrm{T}}}{\partial \mathbf{p}_j}\right]\mathbf{L}_{js} + \frac{\partial \mathbf{p}_{\mathrm{mes}}^{\mathrm{T}}}{\partial \mathbf{p}_j}\mathbf{P}_v^{-1}(\mathbf{z} - \mathbf{p}_{\mathrm{mes}}) \tag{22}$$

$$\mathbf{A}^{\mathrm{T}}\mathbf{L}_{Mp} = \left[\frac{\partial\left[\mathbf{F}\mathbf{S}_{M-1}\right]^{\mathrm{T}}}{\partial \mathbf{p}_M} + \frac{\partial \mathbf{g}^{\mathrm{T}}}{\partial \mathbf{p}_M}\right]\mathbf{L}_{Ms} + \frac{\partial \mathbf{p}_{\mathrm{mes}}^{\mathrm{T}}}{\partial \mathbf{p}_M}\mathbf{P}_v^{-1}(\mathbf{z} - \mathbf{p}_{\mathrm{mes}}) \tag{23}$$

$$\mathbf{L}_{js} = \left[\mathbf{F}^{\mathrm{T}} + \frac{\partial \mathbf{g}^{\mathrm{T}}}{\partial \mathbf{S}_j} + \frac{\partial\left[\mathbf{F}\mathbf{S}_j\right]^{\mathrm{T}}}{\partial \mathbf{S}_j}\right]\mathbf{L}_{(j+1)s} - \left[\frac{\partial[\mathbf{A}\mathbf{p}_{j+1}]^{\mathrm{T}}}{\partial \mathbf{S}_j} - \frac{\partial[\mathbf{B}\mathbf{p}_j]^{\mathrm{T}}}{\partial \mathbf{S}_j} - \frac{\partial \mathbf{d}^{\mathrm{T}}}{\partial \mathbf{S}_j}\right]\mathbf{L}_{(j+1)p} \tag{24}$$

$$\mathbf{L}_{Ms} = 0 \tag{25}$$

$$\mathbf{k} = \bar{\mathbf{k}} - \mathbf{P}_k\left(\sum_{j=1}^{M}\left\{\frac{\partial\left[\mathbf{A}\mathbf{p}_j\right]^{\mathrm{T}}}{\partial \mathbf{k}}\mathbf{L}_{jp} - \frac{\partial \mathbf{d}^{\mathrm{T}}}{\partial \mathbf{k}}\mathbf{L}_{jp} - \frac{\partial\left[\mathbf{F}\mathbf{S}_{j-1}\right]^{\mathrm{T}}}{\partial \mathbf{k}}\mathbf{L}_{js} - \frac{\partial \mathbf{g}^{\mathrm{T}}}{\partial \mathbf{k}}\mathbf{L}_{js}\right\}\right) \tag{26}$$

$$\mathbf{A}\mathbf{p}_j = \mathbf{B}\mathbf{p}_{j-1} + \mathbf{d} + \boldsymbol{\epsilon}_j \tag{27}$$

$$\boldsymbol{\epsilon}_j = \mathbf{P}_{\epsilon_j}\mathbf{L}_{jp} \tag{28}$$

$$\mathbf{p}_0 = \mathbf{p}_{\mathrm{init}} \tag{29}$$

$$\mathbf{S}_j = \mathbf{F}\mathbf{S}_{j-1} + \mathbf{g} + \mathbf{w}_j \tag{30}$$

$$\mathbf{w}_j = \mathbf{P}_{w_j}\mathbf{L}_{js} \tag{31}$$

$$\mathbf{S}_0 = \mathbf{S}_{\mathrm{init}} \tag{32}$$

The Euler–Lagrange equations are coupled. The backward model depends on the optimal solution for pressure (equation 22 and 23). Therefore, we cannot first solve the backward model followed by solving a forward model. The two-point boundary value problem can, however, be solved with the help of the representer method introduced by Bennett [3]. Because the Euler–Lagrange equations are nonlinear, Valstar's [14] extension of Bennett's method was adapted in this study.

3.2 The representer method

The method used in this section is based on the derivation given in [14].

In the representer approach, each unknown variable is expanded in a finite sum of unknown functions (representers), weighted by the representer coefficients. The number of representers equals the number of measurements available.

A representer function describes how the information of the corresponding measurement influences the solution, whereas the representer coefficients determine how strong each representer should be accounted for in the final solution. They depend on the model–data misfit and the prior covariance of data errors. The representer algorithm as introduced in [3] assumes the linearity of the dynamics and observing systems. In that case, the representer expansions will give an exact solution to Euler–Lagrange equations. If this condition is not satisfied, the method can still be applied, but then it only gives an approximate solution.

For a reservoir model, the representer expansions for the adjoint variables (Lagrange multipliers), parameters, and state variables take the following form:

$$\mathbf{L}_{jp} = \sum_{p=1}^{N}\Phi_p(j)b_p \tag{33}$$

$$\mathbf{L}_{js} = \sum_{p=1}^{N}\Gamma_p(j)b_p \tag{34}$$

$$\mathbf{k} = \bar{\mathbf{k}} + \sum_{p=1}^{N}\Psi_p b_p \tag{35}$$

$$\mathbf{S}_j = \mathbf{S}_{F_j} + \mathbf{S}_{\mathrm{corr}_j} + \sum_{p=1}^{N} \Omega_p(j) b_p \tag{36}$$

$$\mathbf{p}_j = \mathbf{p}_{F_j} + \mathbf{p}_{\mathrm{corr}_j} + \sum_{p=1}^{N} \Xi_p(j) b_p, \tag{37}$$

where $\Phi_p(j)$ is the pressure adjoint representer for measurement p, $\Gamma_p(j)$ is the saturation adjoint representer, Ψ_p is the parameter representer, $\Omega_p(j)$ is the saturation representer, and $\Xi_p(j)$ is the pressure representer. b_p are unknown representer coefficients. $\mathbf{S}_{F_j}$ and $\mathbf{p}_{F_j}$ are the forward solutions for saturation and pressure, respectively, obtained without model errors and with parameter $\mathbf{k}$ equal to its prior mean $\bar{\mathbf{k}}$. $\mathbf{S}_{\mathrm{corr}_j}$ and $\mathbf{p}_{\mathrm{corr}_j}$ are the correction terms, and N denotes the number of measurements available.

Because the reservoir model considered here is nonlinear, an iterative scheme was used to obtain a solution. Each of the nonlinear terms was approximated by its first-order Taylor expansion around the estimate obtained from the previous iteration. The resulting linearized Euler–Lagrange equations were solved, the unknowns updated, and iteration repeated until convergence.

By inserting the representer expansions into linearized Euler–Lagrange equations, one can decouple the system and solve iteratively for representers, correction terms, and parameters. The detailed derivation for our reservoir model can be found in [11] and, for groundwater flow problems, in [14].

The iterative procedure is initialized with all the variables equal to their prior means, i.e. $\mathbf{p}_j = \mathbf{p}_{F_j}$, $\mathbf{S}_j = \mathbf{S}_{F_j}$, $\mathbf{k} = \bar{\mathbf{k}}$, $\mathbf{L}_{jp} = 0$, and $\mathbf{L}_{js} = 0$. Then the representers can be found from:

$$\mathbf{A}^{\mathrm{T}} \Phi_p^{\eta}(j) = \mathbf{B}^{\mathrm{T}} \Phi_p^{\eta}(j+1) + \left[\frac{\partial \left[\mathbf{F}\mathbf{S}_{j-1}\right]^{\mathrm{T}}}{\partial \mathbf{p}_j} + \frac{\partial \mathbf{g}^{\mathrm{T}}}{\partial \mathbf{p}_j}\right] \Gamma_p^{\eta}(j) + \left(\frac{\partial p_{\mathrm{mes}}}{\partial \mathbf{p}_j}\right)^{\mathrm{T}} \tag{38}$$

$$\mathbf{A}^{\mathrm{T}} \Phi_p^{\eta}(M) = \left[\frac{\partial \left[\mathbf{F}\mathbf{S}_{M-1}\right]^{\mathrm{T}}}{\partial \mathbf{p}_M} + \frac{\partial \mathbf{g}^{\mathrm{T}}}{\partial \mathbf{p}_M}\right] \Gamma_p^{\eta}(M) + \left(\frac{\partial p_{\mathrm{mes}}}{\partial \mathbf{p}_M}\right)^{\mathrm{T}} \tag{39}$$

$$\Gamma_p^{\eta}(j) = \left[\mathbf{F}^{\mathrm{T}} + \frac{\partial \mathbf{g}^{\mathrm{T}}}{\partial \mathbf{S}_j} + \frac{\partial \left[\mathbf{F}\mathbf{S}_j\right]^{\mathrm{T}}}{\partial \mathbf{S}_j}\right] \Gamma_p^{\eta}(j+1) - \left[\frac{\partial \left[\mathbf{A}\mathbf{p}_{j+1}\right]^{\mathrm{T}}}{\partial \mathbf{S}_j} - \frac{\partial \left[\mathbf{B}\mathbf{p}_j\right]^{\mathrm{T}}}{\partial \mathbf{S}_j} - \frac{\partial \mathbf{d}^{\mathrm{T}}}{\partial \mathbf{S}_j}\right] \Phi_p^{\eta}(j+1) \tag{40}$$

$$\Gamma_p^{\eta}(M) = 0 \tag{41}$$

$$\Psi_p^{\eta} = -\mathbf{P}_k \sum_{j=1}^{M} \left\{ \left[\frac{\partial \left[\mathbf{A}\mathbf{p}_j\right]^{\mathrm{T}}}{\partial \mathbf{k}} - \frac{\partial \mathbf{d}^{\mathrm{T}}}{\partial \mathbf{k}}\right] \Phi_p^{\eta}(j) - \left[\frac{\partial \left[\mathbf{F}\mathbf{S}_{j-1}\right]^{\mathrm{T}}}{\partial \mathbf{k}} + \frac{\partial \mathbf{g}^{\mathrm{T}}}{\partial \mathbf{k}}\right] \Gamma_p^{\eta}(j) \right\} \tag{42}$$

$$\mathbf{A}\Xi_p^{\eta}(j) = \mathbf{B}\Xi_p^{\eta}(j-1) + \left[\frac{\partial \mathbf{d}}{\partial \mathbf{k}} - \frac{\partial \left[\mathbf{A}\mathbf{p}_j\right]}{\partial \mathbf{k}}\right] \Psi_p^{\eta} + \left[\frac{\partial \left[\mathbf{B}\mathbf{p}_{j-1}\right]}{\partial \mathbf{S}_{j-1}} + \frac{\partial \mathbf{d}}{\partial \mathbf{S}_{j-1}} - \frac{\partial \left[\mathbf{A}\mathbf{p}_j\right]}{\partial \mathbf{S}_{j-1}}\right] \Omega_p^{\eta}(j-1) + \mathbf{P}_{\epsilon_j} \Phi_p^{\eta}(j) \tag{43}$$

$$\Xi_p(0) = 0 \tag{44}$$

$$\Omega_p^{\eta}(j) = \left[\frac{\partial \left[\mathbf{F}\mathbf{S}_{j-1}\right]}{\partial \mathbf{p}_j} + \frac{\partial \mathbf{g}}{\partial \mathbf{p}_j}\right] \Xi_p^{\eta}(j) + \left[\frac{\partial \left[\mathbf{F}\mathbf{S}_{j-1}\right]}{\partial \mathbf{k}} + \frac{\partial \mathbf{g}}{\partial \mathbf{k}}\right] \Psi_p^{\eta} + \left[\mathbf{F} + \frac{\partial \left[\mathbf{F}\mathbf{S}_{j-1}\right]}{\partial \mathbf{S}_{j-1}} + \frac{\partial \mathbf{g}}{\partial \mathbf{S}_{j-1}}\right] \Omega_p^{\eta}(j-1) + \mathbf{P}_{w_j} \Gamma_p^{\eta}(j) \tag{45}$$

$$\Omega_p(0) = 0, \tag{46}$$

where η denotes iteration index.

All the representers are calculated for each measurement. The correction terms for pressures and saturations are updated from:

$$\mathbf{A}\mathbf{p}_{\mathrm{corr}_j}^{\eta} = \mathbf{B}\mathbf{p}_{\mathrm{corr}_{j-1}}^{\eta} + \mathbf{B}\mathbf{p}_{F_{j-1}} - \mathbf{A}\mathbf{p}_{F_j} + \mathbf{d} - \left\{ \left[\frac{\partial \mathbf{d}}{\partial \mathbf{k}} - \frac{\partial \left[\mathbf{A}\mathbf{p}_j\right]}{\partial \mathbf{k}}\right] (\mathbf{k} - \bar{\mathbf{k}}) + \left[\frac{\partial \left[\mathbf{B}\mathbf{p}_{j-1}\right]}{\partial \mathbf{S}_{j-1}} + \frac{\partial \mathbf{d}}{\partial \mathbf{S}_{j-1}} - \frac{\partial \left[\mathbf{A}\mathbf{p}_j\right]}{\partial \mathbf{S}_{j-1}}\right] \times \left(\mathbf{S}_{j-1} - \mathbf{S}_{F_{j-1}} - \mathbf{S}_{\mathrm{corr}_{j-1}}\right) \right\} \tag{47}$$

$$\mathbf{p}_{\mathrm{corr}_0} = 0 \tag{48}$$

$$\mathbf{S}^{\eta}_{\mathrm{corr}_j} = \mathbf{FS}^{\eta}_{\mathrm{corr}_{j-1}} + \mathbf{FS}_{F_{j-1}} - \mathbf{S}_{F_j} + \mathbf{g} - \left\{ \left[\frac{\partial \left[\mathbf{FS}_{j-1}\right]}{\partial \mathbf{k}} + \frac{\partial \mathbf{g}}{\partial \mathbf{k}} \right] (\mathbf{k} - \bar{\mathbf{k}}) + \left[\frac{\partial \left[\mathbf{FS}_{j-1}\right]}{\partial \mathbf{p}_j} + \frac{\partial \mathbf{g}}{\partial \mathbf{p}_j} \right] (\mathbf{p}_j - \mathbf{p}_{F_j} - \mathbf{p}_{\mathrm{corr}_j}) + \left[\frac{\partial \left[\mathbf{FS}_{j-1}\right]}{\partial \mathbf{S}_{j-1}} + \frac{\partial \mathbf{g}}{\partial \mathbf{S}_{j-1}} \right] \times \left(\mathbf{S}_{j-1} - \mathbf{S}_{F_{j-1}} - \mathbf{S}_{\mathrm{corr}_{j-1}}\right) \right\} \quad (49)$$

$$\mathbf{S}_{\mathrm{corr}_0} = 0, \quad (50)$$

and the representer coefficients can be calculated from:

$$(\mathbf{P}_v + \Xi^{\eta}_p)\mathbf{b}^{\eta}_p = \left[\mathbf{z} - (\mathbf{p}_{F_{\mathrm{mes}}} + \mathbf{p}^{\eta}_{\mathrm{corr}_{\mathrm{mes}}})\right]. \quad (51)$$

All the derivatives, matrices, and vectors depending either on pressure, saturation, or permeability are evaluated with the estimates of those variables from the previous iteration $\eta - 1$.

After all the representers, correction terms, and representer coefficients have been obtained, we can update adjoint variables and parameters via their representer expansions 33–35. The updated pressures and saturations are calculated from 27–32, and iteration proceeds until convergence.

4 Application to a reservoir model

The performance of the representer method derived in the previous sections was tested with a synthetic example. This twin experiment can be used to validate the method, as it can be compared with the "real" generated output. For the representer method, all the covariance matrices and the prior mean of parameters are assumed to be known. For this experiment, they were defined by a modeler.

The permeability field and the error fields were generated from the multivariate normal distribution with given means and covariance matrices (see Appendices). The error terms were regarded as uncorrelated in space and time. For permeability, the spatial correlation with exponential structure was introduced.

For the model described by equations 1–11, the constant values for the oil, water, and rock compressibilities, for the diffusion coefficient, and also for the water and oil viscosities were used. The corresponding values have been summarized in Tables 1, 2, and 3.

The relative permeability curves were simulated according to the Corey model. For the forward model, the mean value of the absolute permeability was set to $k = 10^{-13}$ m^2.

The measurements were sampled from the real pressure distribution, with synthetic measurement errors added to those values.

In the assimilation process, only one, two, or three measurements were used. Convergence was achieved when the differences between the measurement predictions from the representer expansion and the measurement predictions from the forward model evaluated with the updated parameters were smaller than 1% of the measurement standard deviation.

The distributions of the pressure and saturation generated are shown in Fig. 1.

Figure 2 shows the adjoint pressure and saturation representers obtained during the first iteration.

The shape of the representer functions is given by the equations presented in previous sections. The pressure adjoint representer satisfies the adjoint pressure equation, except being forced only with a single impulse located at the space–time position of the pth measurement. It shows at which location the additional driving force would influence the model

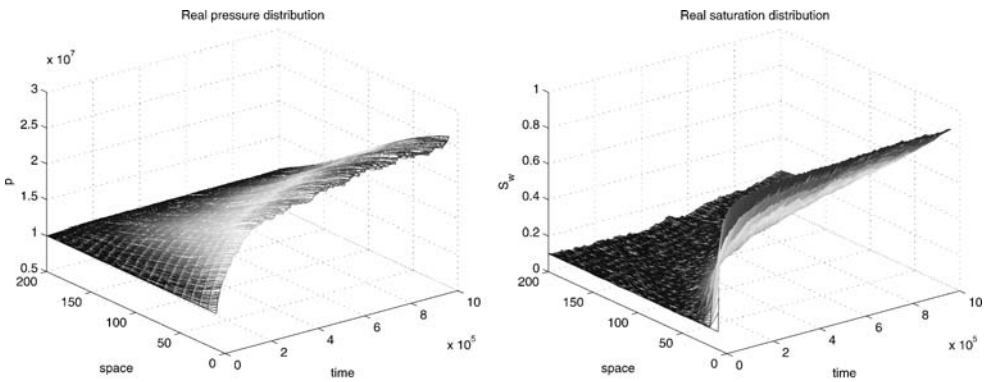

a. Pressure distribution. b. Saturation distribution.

Fig. 1 Real pressure and saturation distributions after 11 days

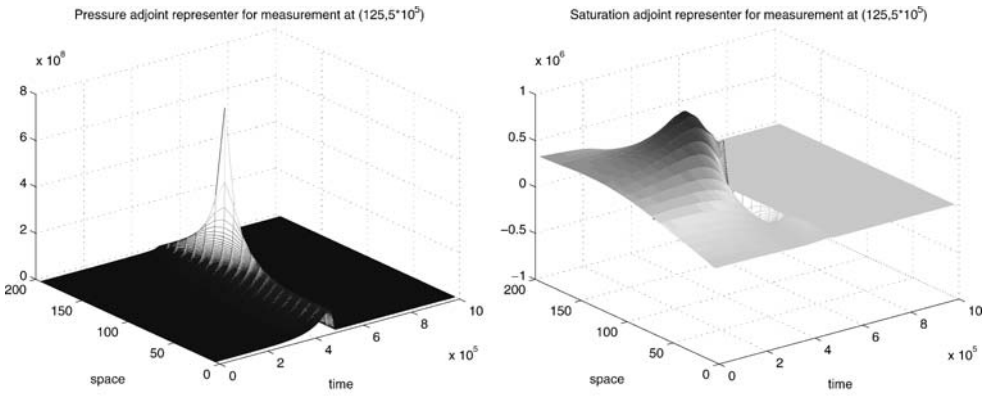

a. Pressure adjoint representer. b. Saturation adjoint representer.

Fig. 2 The pressure and saturation adjoint representers for measurement located at (125m, 5×10^5s)

most. It is maximum at the location of the measurement to which it belongs. The adjoint pressure and saturation representers are coupled, and the shape of saturation adjoint representer is determined by the pressure adjoint representer. Therefore, even though no saturation measurements were available, the saturation adjoint representer appears in the calculations. The parameter representers for two different measurements are shown in Fig. 3.

The parameter representer denotes the shape of the parameter field that can adapt the model prediction of the measurement most efficiently. The parameter was allowed to vary only in space, but the optimal estimate for this parameter depends on the number and location of all measurements used in the assimilation process.

The pressure and saturation representers are shown in Fig. 4. The state variable representers show how the state variables will change if the parameters and model errors are adapted according to their representers fields. The pressure and saturation representers for reservoir model are coupled and have to be solved sequentially.

We were mostly concerned with the estimation of uncertain parameter k. For this purpose, only one, two, or three generated measurements were used. The algorithm converged in two to five iterations depending on the number and location of measurements used. Figure 5 illustrates the convergence behavior during the iteration process, expressed in terms of the L^2 - norm of the difference between the "true" and the estimated permeability values.

The estimated permeability distribution using two measurements is shown in Fig. 6.

If we compare the estimates obtained with one measurement to the "true" permeability, we see significant differences. Both estimates differ from the real k, but

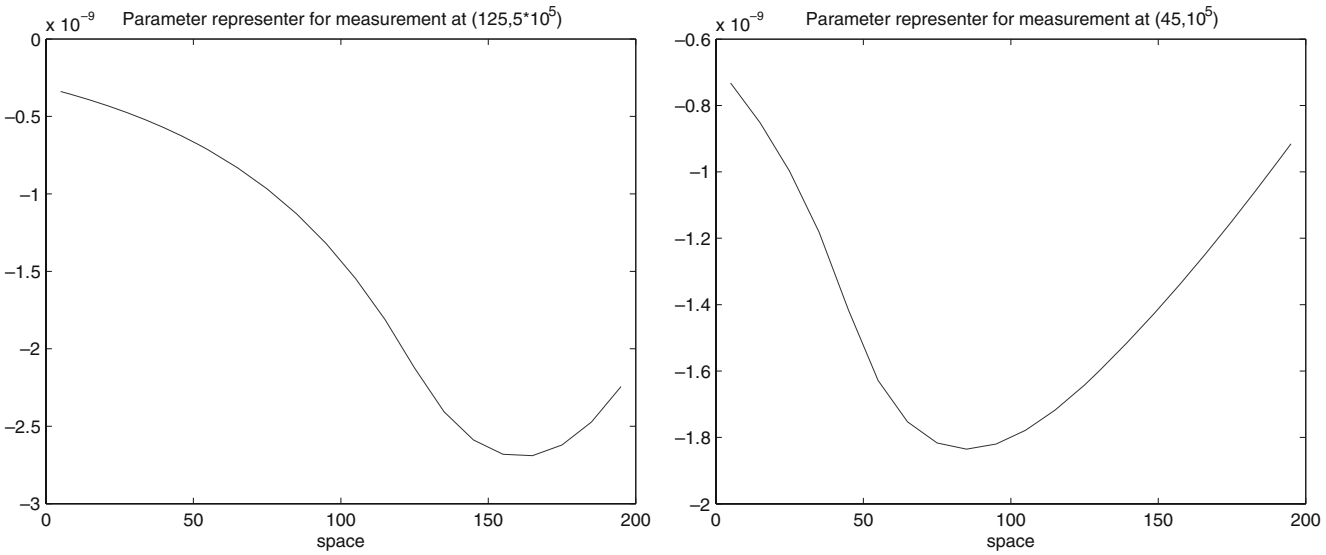

Fig. 3 The permeability representers for different measurement locations

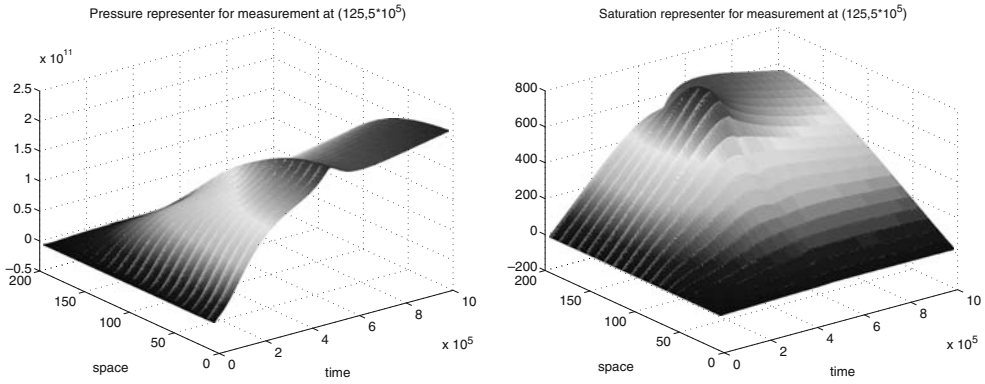

Fig. 4 The pressure and saturation representers for measurement located at (125m, 5×10^5s)

a. Pressure representer. b. Saturation representer.

approximate it much better than the mean value. The estimate obtained with two measurements shows the most improvement.

The estimation results for a case where three measurements were used in the estimation process are shown in Fig. 7. For comparison, the separate estimates obtained with each of the measurements are shown as well.

The permeability estimates are clearly improved compared to the prior value, as illustrated in Fig. 5. For this experiment, measurements were sampled in space at distant locations. In this way, a better estimate of permeability was obtained compared with the case where measurements were sampled at small distances (Fig. 6).

The estimates obtained with one measurement introduce only small improvements, as was expected, because it is hard to obtain all relevant information about permeability in the whole domain from only one measurement. The permeability estimate obtained with three measurements resembles the "true" permeability distribution, although there are still significant differences.

The state variables were estimated together with the parameters. The results are not shown here, as they are not visible on graphs of estimates.

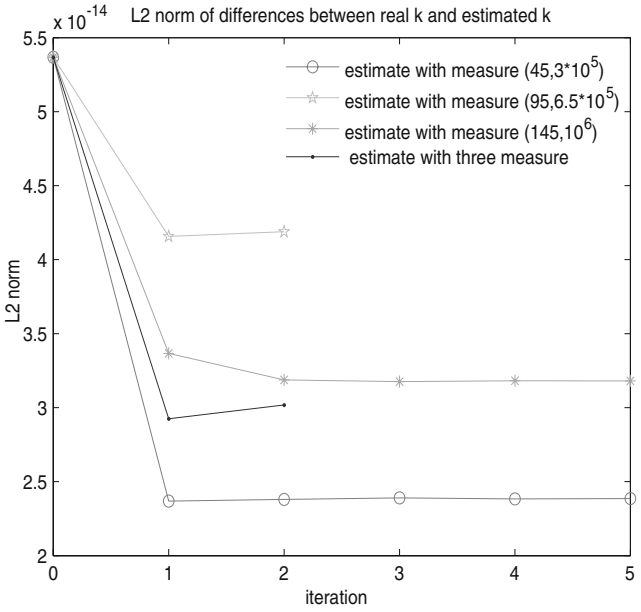

Fig. 5 L^2 - norm of the difference between the "true" and the estimated permeability values

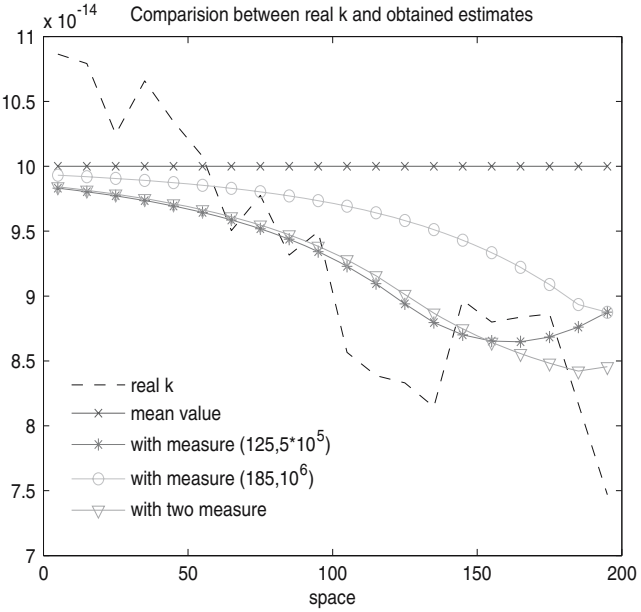

Fig. 6 Comparison between generated permeability k and estimates obtained with one and two measurements

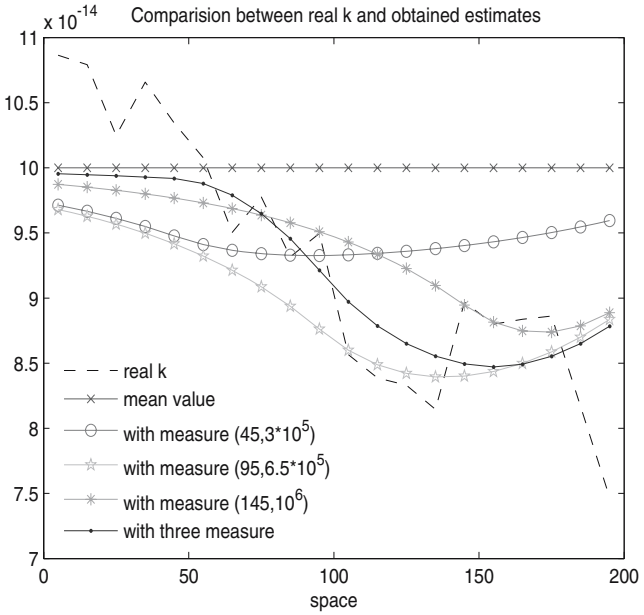

Fig. 7 Comparison between generated permeability k and estimates obtained with one and three measurements

5 Conclusions

This study successfully used the representer method to estimate states and parameters for a simple, but nonlinear, 1-D reservoir model. The representer method uses an optimal parametrization by defining representers for all measurements. It allows the number of independent estimation parameters to be reduced to the number of measurements while still providing a solution to the full inverse problem. The method is computationally attractive if the number of measurements is relatively small compared to the number of unknown parameters. To apply the representer method, the statistics of the uncertain parameters and the measurements have to be known. In this paper, all statistics were set by the modeler and used to generate "true" fields for pressure and saturation. From the pressure field, measurements were sampled, to which an additional measurement error was added. Estimates obtained using the inverse approach were compared with the "true" fields. During estimation, only one, two, or three measurements (discrete in time and space) were used. This number of measurements is too small to obtain the information about variables in the entire domain but still yielded acceptable estimates. These results indicate that the representer method is a promising tool for data assimilation in uncertain reservoir models. The next step should be to implement the representer method in a more realistic reservoir model with suitable chosen statistics for model errors and parameters.

Acknowledgement The authors would like to thank Johan Valstar for his advice during the research.

Appendix

Appendix A: Derivation of forward model

This appendix contains the derivation of governing equations for two-phase (oil–water) flow in one dimension. As shown in [1], a two-phase flow system can be expressed in terms of oil pressure p_o and water saturation S as follows:

$$
\begin{aligned}
&-\nabla\cdot\left\{\frac{\alpha\rho_w k_{rw}}{\mu_w}\mathbf{K}\left[\left(\nabla p_o-\frac{\partial p_c}{\partial S}\nabla S\right)-\rho_w g\nabla d\right]\right\}\\
&\quad+\alpha\rho_w\phi\left[S(c_w+c_r)\frac{\partial p_o}{\partial t}+\frac{\partial S}{\partial t}\right]\\
&\quad-\alpha\rho_w q_w'''=0 \qquad (52)\\
&-\nabla\cdot\left[\frac{\alpha\rho_o k_{ro}}{\mu_o}\mathbf{K}\left(\nabla p_o-\rho_o g\nabla d\right)\right]\\
&\quad+\alpha\rho_o\phi\left[(1-S)(c_o+c_r)\frac{\partial p_o}{\partial t}-\frac{\partial S}{\partial t}\right]\\
&\quad-\alpha\rho_o q_o'''=0 \qquad (53)
\end{aligned}
$$

where α is a geometric factor that accounts for different dimensions, ρ_w and ρ_o are water and oil densities, μ_w and μ_o are water and oil viscosities, and c_w, c_o, and c_r are water, oil, and rock compressibilities, respectively. $\mathbf{K}$ stands for permeability tensor, p_c denotes capillary pressure, and q_w''' and q_o''' are water and oil flow rates, respectively.

Introducing a simplification in which the nonlinear diffusive effect of the capillary pressure is replaced by a linear diffusion –dispersion coefficient D, the equations are simplified to:

$$
\begin{aligned}
&-\nabla\cdot\left[\frac{\alpha\rho_w k_{rw}}{\mu_w}\mathbf{K}\left(\nabla p-\rho_w g\nabla d\right)\right]\\
&\quad+\alpha\rho_w D\nabla^2 S+\alpha\rho_w\phi\left[S(c_w+c_r)\frac{\partial p}{\partial t}+\frac{\partial S}{\partial t}\right]\\
&\quad-\alpha\rho_w q_w'''=0 \qquad (54)\\
&-\nabla\cdot\left[\frac{\alpha\rho_o k_{ro}}{\mu_o}\mathbf{K}\left(\nabla p-\rho_o g\nabla d\right)\right]\\
&\quad+\alpha\rho_o\phi\left[(1-S)(c_o+c_r)\frac{\partial p}{\partial t}-\frac{\partial S}{\partial t}\right]\\
&\quad-\alpha\rho_o q_o'''=0 \qquad (55)
\end{aligned}
$$

The subscript "o" has been dropped for the pressure because the absence of capillary pressure implies $p_o = p_w$.

The nature of two-phase flow equations is discussed in [1] and [10]. The pressure behavior is essentially diffusive, i.e. the corresponding equations are parabolic and become elliptic in the limit of zero compressibility. The saturation behavior is mixed diffusive–convective, i.e. the corresponding equations are mixed parabolic–hyperbolic and become completely hyperbolic in the case of zero capillary pressure.

This can be seen by rewriting two-phase flow equations for 1-D flow through a conduit with unit cross-sectional area. For small compressibilities such that we may assume that ρ is constant but c finite, in the absence of gravity terms and capillary pressure and source terms, and with isotropic permeability k, the corresponding equations take the form:

$$-\frac{\partial}{\partial x}\left(\lambda_w \frac{\partial p}{\partial x}\right) + \phi\left[S(c_w + c_r)\frac{\partial p}{\partial t} + \frac{\partial S}{\partial t}\right] = 0 \quad (56)$$

$$-\frac{\partial}{\partial x}\left(\lambda_o \frac{\partial p}{\partial x}\right) + \phi\left[(1-S)(c_o + c_r)\frac{\partial p}{\partial t} - \frac{\partial S}{\partial t}\right] = 0 \quad (57)$$

Here we introduced the water and oil mobilities:

$$\lambda_w = \frac{k k_{rw}(S)}{\mu_w} \text{ and } \lambda_o = \frac{k k_{ro}(S)}{\mu_o} \quad (58)$$

Adding equations 56–57 results in a PDE with only the pressure as primary variable (and coefficients being function of saturation):

$$-\frac{\partial}{\partial x}\left(\lambda_t \frac{\partial p}{\partial x}\right) + \phi c_t \frac{\partial p}{\partial t} = 0 \quad (59)$$

where the total mobility λ_t and the total compressibility c_t have been defined as:

$$\lambda_t = \lambda_w + \lambda_o \quad (60)$$

$$c_t = c_r + S c_w + (1-S)c_o \quad (61)$$

Equation 59 is a parabolic equation with non-constant coefficients.

Another equation, describing the evolution of water saturation can bo obtained in the following way.

From Darcy's law we have:

$$\mathbf{v}_w = -\frac{\mathbf{K} k_{rw}}{\mu_w}\left(\nabla p_w - \rho_w g \nabla d\right) \quad (62)$$

with $\mathbf{v}_w$ superficial water velocity.

From continuity equation for single-phase flow, we have:

$$-\nabla \cdot \left(\alpha \rho_w \mathbf{v}_w\right) + \alpha \rho_w q_w''' = \alpha \frac{\partial\left(\rho_w \phi S\right)}{\partial t} \quad (63)$$

Defining total velocity as:

$$\mathbf{v} = \mathbf{v}_w + \mathbf{v}_o \quad (64)$$

and fractional flow function as:

$$f_w = \frac{\lambda_w}{\lambda_w + \lambda_o} \quad (65)$$

after some calculations, we arrive at [10]:

$$\frac{1}{\alpha}\nabla \cdot \left(\alpha h_w \nabla S\right) - \frac{\mathrm{d} f_w}{\mathrm{d} S}\mathbf{v} \cdot \nabla S = \phi \frac{\partial S}{\partial t} + \frac{1}{\alpha}\nabla \cdot \left(\alpha G_w \nabla d\right) \quad (66)$$

with h_w and G_w defined as:

$$h_w = -\frac{\lambda_o \lambda_w}{\lambda_o + \lambda_w}\frac{\mathrm{d} p_c}{\mathrm{d} S} \text{ and } G_w = f_w \lambda_o (\rho_w - \rho_o) g \quad (67)$$

In 1-D flow, neglecting gravity terms and replacing the nonlinear diffusive effect of capillary pressure by a diffusion coefficient D, we obtain for unit cross-sectional area:

$$D\frac{\partial^2 S}{\partial x} - v\frac{\mathrm{d} f_w}{\mathrm{d} S}\frac{\partial S}{\partial x} = \phi \frac{\partial S}{\partial t} \quad (68)$$

This equation is a nonlinear version of diffusion–convection equation:

$$D\frac{\partial^2 C}{\partial x} - v_t \frac{\partial C}{\partial x} = \phi \frac{\partial C}{\partial t} \quad (69)$$

where D is diffusivity and C stands for concentration.

This diffusion–convection equation was used to approximate the evolution of water saturation in this paper.

Appendix B: Euler–Lagrange equations – derivation

The objective function (21) is augmented by adding the pressure and saturation equations multiplied by 2 times the adjoint variables $\mathbf{L}_{jp}$ and $\mathbf{L}_{js}$, respectively:

$$\begin{aligned}\mathcal{J} = {} & (\mathbf{z} - \mathbf{p}_{mes})^T \mathbf{P}_v^{-1}(\mathbf{z} - \mathbf{p}_{mes}) + (\mathbf{k} - \bar{\mathbf{k}})^T \mathbf{P}_k^{-1}(\mathbf{k} - \bar{\mathbf{k}}) \\ & + \sum_{j=1}^{M} \boldsymbol{\epsilon}_j^T \mathbf{P}_{\epsilon_j}^{-1} \boldsymbol{\epsilon}_j + \sum_{j=1}^{M} \mathbf{w}_j^T \mathbf{P}_{w_j}^{-1} \mathbf{w}_j \\ & + 2\sum_{j=1}^{M} \mathbf{L}_{jp}^T \left[\mathbf{A}\mathbf{p}_j - \mathbf{B}\mathbf{p}_{j-1} - \mathbf{d} - \boldsymbol{\epsilon}_j\right] \\ & + 2\sum_{j=1}^{M} \mathbf{L}_{js}^T \left[\mathbf{S}_j - \mathbf{F}\mathbf{S}_{j-1} - \mathbf{g} - \mathbf{w}_j\right] \end{aligned} \quad (70)$$

Taking the first variation with respect to pressures, saturations, parameters, error terms, and adjoint variables (Lagrange multipliers) yields:

$$\frac{1}{2}\Delta\mathcal{J} = \frac{1}{2}\frac{\partial\mathcal{J}}{\partial\mathbf{k}}\Delta\mathbf{k} + \frac{1}{2}\sum_{j=0}^{M}\frac{\partial\mathcal{J}}{\partial\mathbf{p}_j}\Delta\mathbf{p}_j + \frac{1}{2}\sum_{j=0}^{M}\frac{\partial\mathcal{J}}{\partial\mathbf{S}_j}\Delta\mathbf{S}_j + \frac{1}{2}\sum_{j=1}^{M}\frac{\partial\mathcal{J}}{\partial\boldsymbol{\epsilon}_j}\Delta\boldsymbol{\epsilon}_j + \frac{1}{2}\sum_{j=1}^{M}\frac{\partial\mathcal{J}}{\partial\mathbf{w}_j}\Delta\mathbf{w}_j + \frac{1}{2}\sum_{j=1}^{M}\frac{\partial\mathcal{J}}{\partial\mathbf{L}_{jp}}\Delta\mathbf{L}_{jp} + \frac{1}{2}\sum_{j=1}^{M}\frac{\partial\mathcal{J}}{\partial\mathbf{L}_{js}}\Delta\mathbf{L}_{js}. \tag{71}$$

In the minimum of the penalty function, the first variation vanishes for any variation of variables. Thus, setting the appropriate derivatives to zero, we get a system of Euler–Lagrange equations.

For the variation of pressures $\Delta\mathbf{p}_j$, it gives the adjoint system for pressures:

$$\mathbf{A}^{\mathrm{T}}\mathbf{L}_{jp} = \mathbf{B}^{\mathrm{T}}\mathbf{L}_{(j+1)p} + \left[\frac{\partial\left[\mathbf{F}\mathbf{S}_{j-1}\right]^{\mathrm{T}}}{\partial\mathbf{p}_j} + \frac{\partial\mathbf{g}^{\mathrm{T}}}{\partial\mathbf{p}_j}\right]\mathbf{L}_{js} + \frac{\partial\mathbf{p}_{\mathrm{mes}}^{\mathrm{T}}}{\partial\mathbf{p}_j}\mathbf{P}_v^{-1}(\mathbf{z}-\mathbf{p}_{\mathrm{mes}}) \quad \text{for } j = M-1, ..., 1 \tag{72}$$

$$\mathbf{A}^{\mathrm{T}}\mathbf{L}_{Mp} = \left[\frac{\partial\left[\mathbf{F}\mathbf{S}_{M-1}\right]^{\mathrm{T}}}{\partial\mathbf{p}_M} + \frac{\partial\mathbf{g}^{\mathrm{T}}}{\partial\mathbf{p}_M}\right]\mathbf{L}_{Ms} + \frac{\partial\mathbf{p}_{\mathrm{mes}}^{\mathrm{T}}}{\partial\mathbf{p}_M}\mathbf{P}_v^{-1}(\mathbf{z}-\mathbf{p}_{\mathrm{mes}}). \tag{73}$$

For the variation of saturations $\Delta\mathbf{S}_j$, it gives the adjoint system for saturations:

$$\mathbf{L}_{js} = \left[\mathbf{F}^{\mathrm{T}} + \frac{\partial\mathbf{g}^{\mathrm{T}}}{\partial\mathbf{S}_j} + \frac{\partial\left[\mathbf{F}\mathbf{S}_j\right]^{\mathrm{T}}}{\partial\mathbf{S}_j}\right]\mathbf{L}_{(j+1)s} - \left[\frac{\partial[\mathbf{A}\mathbf{p}_{j+1}]^{\mathrm{T}}}{\partial\mathbf{S}_j} - \frac{\partial[\mathbf{B}\mathbf{p}_j]^{\mathrm{T}}}{\partial\mathbf{S}_j} - \frac{\partial\mathbf{d}^{\mathrm{T}}}{\partial\mathbf{S}_j}\right]\mathbf{L}_{(j+1)p} \quad \text{for } j = M-1, ..., 1 \tag{74}$$

$$\mathbf{L}_{Ms} = 0. \tag{75}$$

where the expression $\frac{\partial\left[\mathbf{F}\mathbf{S}_j\right]^{\mathrm{T}}}{\partial\mathbf{S}_j}$ denotes the derivative with respect to $\mathbf{S}_{j-1}$ of coefficients of matrix $\mathbf{F}$.

For the variation of parameters $\Delta\mathbf{k}$, it yields the parameter equation:

$$\mathbf{k} = \bar{\mathbf{k}} - \mathbf{P}_k\left(\sum_{j=1}^{M}\left\{\frac{\partial\left[\mathbf{A}\mathbf{p}_j\right]^{\mathrm{T}}}{\partial\mathbf{k}}\mathbf{L}_{jp} - \frac{\partial\mathbf{d}^{\mathrm{T}}}{\partial\mathbf{k}}\mathbf{L}_{jp} - \frac{\partial\left[\mathbf{F}\mathbf{S}_{j-1}\right]^{\mathrm{T}}}{\partial\mathbf{k}}\mathbf{L}_{js} - \frac{\partial\mathbf{g}^{\mathrm{T}}}{\partial\mathbf{k}}\mathbf{L}_{js}\right\}\right). \tag{76}$$

For the variation of pressure model errors $\Delta\boldsymbol{\epsilon}_j$, it yields the pressure error equation:

$$\boldsymbol{\epsilon}_j = \mathbf{P}_{\epsilon_j}\mathbf{L}_{jp} \quad \text{for } j = 1, ..., M. \tag{77}$$

For the variation of saturation model errors $\Delta\mathbf{w}_j$, it yields the saturation error equation:

$$\mathbf{w}_j = \mathbf{P}_{w_j}\mathbf{L}_{js} \quad \text{for } j = 1, ..., M. \tag{78}$$

For the variation of Lagrange multipliers $\Delta\mathbf{L}_{jp}$ and $\Delta\mathbf{L}_{js}$, it yields the forward model given by equations 12–15.

Appendix C: Representer equations – derivation

Inserting the representer definitions introduced in equations 33–37 into Euler–Lagrange equations, we find the explicit formulas for the representers, correction terms, and representer coefficients.

C.1 Pressure adjoint representer

Inserting representer definitions into pressure adjoint equations 22 and 23 gives:

$$\mathbf{A}^{\mathrm{T}}\Phi_p(j)\mathbf{b}_p = \mathbf{B}\Phi_p(j+1)\mathbf{b}_p + \left[\frac{\partial\left[\mathbf{F}\mathbf{S}_{j-1}\right]^{\mathrm{T}}}{\partial\mathbf{p}_j} + \frac{\partial\mathbf{g}^{\mathrm{T}}}{\partial\mathbf{p}_j}\right] \times \boldsymbol{\Gamma}_p(j)\mathbf{b}_p + \frac{\partial\mathbf{p}_{\mathrm{mes}}^{\mathrm{T}}}{\partial\mathbf{p}_j}\mathbf{P}_v^{-1}\left[\mathbf{z} - (\mathbf{p}_{F_{\mathrm{mes}}} + \mathbf{p}_{\mathrm{corr}_{\mathrm{mes}}} + \Xi_p\mathbf{b}_p)\right] \tag{79}$$

$$\mathbf{A}^{\mathrm{T}}\Phi_p(M)\mathbf{b}_p = \left[\frac{\partial\left[\mathbf{F}\mathbf{S}_{M-1}\right]^{\mathrm{T}}}{\partial\mathbf{p}_M} + \frac{\partial\mathbf{g}^{\mathrm{T}}}{\partial\mathbf{p}_M}\right]\boldsymbol{\Gamma}_p(M)\mathbf{b}_p + \frac{\partial\mathbf{p}_{\mathrm{mes}}^{\mathrm{T}}}{\partial\mathbf{p}_M}\mathbf{P}_v^{-1}\left[\mathbf{z} - (\mathbf{p}_{F_{\mathrm{mes}}} + \mathbf{p}_{\mathrm{corr}_{\mathrm{mes}}} + \Xi_p\mathbf{b}_p)\right] \tag{80}$$

In this stage, both the pressure adjoint representers $\Phi_p(j)$ and coefficients b_p are unknown. Defining coefficients for all measurements as:

$$\mathbf{b}_p = \mathbf{P}_v^{-1}\left[\mathbf{z} - (\mathbf{p}_{F_{\mathrm{mes}}} + \mathbf{p}_{\mathrm{corr}_{\mathrm{mes}}} + \Xi_p\mathbf{b}_p)\right] \tag{81}$$

and inserting this definition into equations 79 and 80, these equations can be fulfilled for nonzero b if the pressure adjoint representer satisfies:

$$\mathbf{A}^{\mathrm{T}}\Phi_p(j) = \mathbf{B}^{\mathrm{T}}\Phi_p(j+1) + \left[\frac{\partial\left[\mathbf{FS}_{j-1}\right]^{\mathrm{T}}}{\partial \mathbf{p}_j} + \frac{\partial \mathbf{g}^{\mathrm{T}}}{\partial \mathbf{p}_j}\right]\Gamma_p(j) + \left(\frac{\partial p_{\mathrm{mes}}}{\partial \mathbf{p}_j}\right)^{\mathrm{T}} \tag{82}$$

$$\mathbf{A}^{\mathrm{T}}\Phi_p(M) = \left[\frac{\partial\left[\mathbf{FS}_{M-1}\right]^{\mathrm{T}}}{\partial \mathbf{p}_M} + \frac{\partial \mathbf{g}^{\mathrm{T}}}{\partial \mathbf{p}_M}\right]\Gamma_p(M) + \left(\frac{\partial p_{\mathrm{mes}}}{\partial \mathbf{p}_M}\right)^{\mathrm{T}}. \tag{83}$$

C.2 Saturation adjoint representer

Inserting representer definitions into saturation adjoint equations 24 and 25 gives:

$$\mathbf{\Gamma}_p(j)\mathbf{b}_p = \left[\mathbf{F}^{\mathrm{T}} + + \frac{\partial \mathbf{g}^{\mathrm{T}}}{\partial \mathbf{S}_j} + \frac{\partial\left[\mathbf{FS}_j\right]^{\mathrm{T}}}{\partial \mathbf{S}_j}\right]\mathbf{\Gamma}_p(j+1)\mathbf{b}_p - \left[\frac{\partial\left[\mathbf{Ap}_{j+1}\right]^{\mathrm{T}}}{\partial \mathbf{S}_j} - \frac{\partial\left[\mathbf{Bp}_j\right]^{\mathrm{T}}}{\partial \mathbf{S}_j} - \frac{\partial \mathbf{d}^{\mathrm{T}}}{\partial \mathbf{S}_j}\right]\Phi_p(j+1)\mathbf{b}_p \tag{84}$$

$$\mathbf{\Gamma}_p(M)\mathbf{b}_p = 0. \tag{85}$$

These equations can be fulfilled for nonzero b if for every measurement p:

$$\Gamma_p(j) = \left[\mathbf{F}^{\mathrm{T}} + \frac{\partial \mathbf{g}^{\mathrm{T}}}{\partial \mathbf{S}_j} + \frac{\partial\left[\mathbf{FS}_j\right]^{\mathrm{T}}}{\partial \mathbf{S}_j}\right]\Gamma_p(j+1) - \left[\frac{\partial\left[\mathbf{Ap}_{j+1}\right]^{\mathrm{T}}}{\partial \mathbf{S}_j} - \frac{\partial\left[\mathbf{Bp}_j\right]^{\mathrm{T}}}{\partial \mathbf{S}_j} - \frac{\partial \mathbf{d}^{\mathrm{T}}}{\partial \mathbf{S}_j}\right]\Phi_p(j+1) \tag{86}$$

$$\Gamma_p(M) = 0. \tag{87}$$

C.3 Parameter representer

Inserting representer definitions into parameter equation 26 gives:

$$\bar{\mathbf{k}} + \Psi_p\mathbf{b}_p = \bar{\mathbf{k}} - \mathbf{P}_k\sum_{j=1}^{M}\left\{\left[\frac{\partial\left[\mathbf{Ap}_j\right]^{\mathrm{T}}}{\partial \mathbf{k}} - \frac{\partial \mathbf{d}^{\mathrm{T}}}{\partial \mathbf{k}}\right]\Phi_p(j)\mathbf{b}_p - \left[\frac{\partial\left[\mathbf{FS}_{j-1}\right]^{\mathrm{T}}}{\partial \mathbf{k}} + \frac{\partial \mathbf{g}^{\mathrm{T}}}{\partial \mathbf{k}}\right]\mathbf{\Gamma}_p(j)\mathbf{b}_p\right\}. \tag{88}$$

This equation can be fulfilled for nonzero b if:

$$\Psi_p = -\mathbf{P}_k\sum_{j=1}^{M}\left\{\left[\frac{\partial\left[\mathbf{Ap}_j\right]^{\mathrm{T}}}{\partial \mathbf{k}} - \frac{\partial \mathbf{d}^{\mathrm{T}}}{\partial \mathbf{k}}\right]\Phi_p(j) - \left[\frac{\partial\left[\mathbf{FS}_{j-1}\right]^{\mathrm{T}}}{\partial \mathbf{k}} + \frac{\partial \mathbf{g}^{\mathrm{T}}}{\partial \mathbf{k}}\right]\Gamma_p(j)\right\}. \tag{89}$$

C.4 Pressure representer

The pressure representers are chosen such that during each iteration, those representers are an exact linearization around the pressure estimate of the previous iteration. The pressure equation is perturbed around the estimate of the previous iteration $n-1$:

$$\begin{aligned}\mathbf{A}\,(\,S_{j-1}^{\eta-1} + \Omega_p(j-1)\delta b_p, k^{\eta-1} + \Psi_p\delta b_p)\\ \times\left[\mathbf{p}_j^{\eta-1} + \Xi_p(j)\delta\mathbf{b}_p\right] = \mathbf{B}(S_{j-1}^{\eta-1} + \Omega_p(j-1)\delta b_p)\\ \times\left[\mathbf{p}_{j-1}^{\eta-1} + \Xi_p(j-1)\delta\mathbf{b}_p\right] + \mathbf{d}(S_{j-1}^{\eta-1} + \Omega_p(j-1)\delta b_p,\\ k^{\eta-1} + \Psi_p\delta b_p) + \boldsymbol{\epsilon}_j^{\eta-1} + \mathbf{P}_{\epsilon_j}\Phi_p(j)\delta\mathbf{b}_p\end{aligned} \tag{90}$$

$$\mathbf{p}_0 + \Xi_p(0)\delta\mathbf{b}_p = \mathbf{p}_{\mathrm{init}}. \tag{91}$$

Linearizing those equations and dividing by δb_p yield the pressure representer for measurement p:

$$\mathbf{A}\Xi_p(j) = \mathbf{B}\Xi_p(j-1) + \left[\frac{\partial\left[\mathbf{Bp}_{j-1}\right]}{\partial \mathbf{S}_{j-1}} + \frac{\partial \mathbf{d}}{\partial \mathbf{S}_{j-1}} - \frac{\partial\left[\mathbf{Ap}_j\right]}{\partial \mathbf{S}_{j-1}}\right]\times\Omega_p(j-1) + \left[\frac{\partial \mathbf{d}}{\partial \mathbf{k}} - \frac{\partial\left[\mathbf{Ap}_j\right]}{\partial \mathbf{k}}\right]\Psi_p + \mathbf{P}_{\epsilon_j}\Phi_p(j) \tag{92}$$

$$\Xi_p(0) = 0. \tag{93}$$

C.5 Pressure correction term

The correction term will be chosen in such a way that the forward pressure equation will be fulfilled. Inserting the representer definitions into the pressure equation yields:

$$\begin{aligned}\mathbf{A}\left[\mathbf{p}_{F_j} + \mathbf{p}_{\mathrm{corr}_j} + \Xi_p(j)\mathbf{b}_p\right] = \mathbf{B}\left[\mathbf{p}_{F_{j-1}} + \mathbf{p}_{\mathrm{corr}_{j-1}}\right.\\ \left. + \Xi_p(j-1)\mathbf{b}_p\right]\\ + \mathbf{d} + \mathbf{P}_{\epsilon_j}\Phi_p(j)\mathbf{b}_p\end{aligned} \tag{94}$$

$$\mathbf{p}_{F_0} + \mathbf{p}_{\mathrm{corr}_0} + \Xi_p(0)\mathbf{b}_p = \mathbf{p}_{\mathrm{init}}. \tag{95}$$

Multiplying equations 92 and 93 by b_p, summing over all N measurements, and inserting into equations 94 and 95 yield after some rearranging:

$$\begin{aligned}\mathbf{Ap}_{\mathrm{corr}_j} = \mathbf{Bp}_{\mathrm{corr}_{j-1}} + \mathbf{Bp}_{F_{j-1}} - \mathbf{Ap}_{F_j} + \mathbf{d} \\ -\left\{\left[\frac{\partial \mathbf{d}}{\partial \mathbf{k}} - \frac{\partial\left[\mathbf{Ap}_j\right]}{\partial \mathbf{k}}\right](\mathbf{k} - \bar{\mathbf{k}}) \right. \\ + \left[\frac{\partial\left[\mathbf{Bp}_{j-1}\right]}{\partial \mathbf{S}_{j-1}} + \frac{\partial \mathbf{d}}{\partial \mathbf{S}_{j-1}} - \frac{\partial\left[\mathbf{Ap}_j\right]}{\partial \mathbf{S}_{j-1}}\right] \\ \left. \times \left(\mathbf{S}_{j-1} - \mathbf{S}_{F_{j-1}} - \mathbf{S}_{\mathrm{corr}_{j-1}}\right)\right\} \qquad (96)\end{aligned}$$

$$\mathbf{p}_{\mathrm{corr}_0} = 0. \qquad (97)$$

C.6 Saturation representer and saturation correction term

The saturation representers and saturation correction terms are derived in the same way as the pressure representers and pressure correction terms.

C.7 Representer coefficients

The representer coefficients were defined in (81). After rearranging this yields the equation:

$$(\mathbf{P}_v + \Xi_p^{\eta})\mathbf{b}_p^{\eta} = \left[\mathbf{z} - (\mathbf{p}_{F_{\mathrm{mes}}} + \mathbf{p}^{\eta}_{\mathrm{corr}_{\mathrm{mes}}})\right]. \qquad (98)$$

This matrix equation can only be solved when all the representers and correction terms have been calculated.

Appendix D: Reservoir description

Table 1 Reservoir description: input data for reservoir model

Porosity (-)	0.2
Oil compressibility (Pa^{-1})	0.3×10^{-8}
Rock compressibility (Pa^{-1})	0
Water compressibility (Pa^{-1})	0.2×10^{-9}
Oil viscosity ($\mathrm{Pa} \cdot s$)	9.8×10^{-4}
Water viscosity ($\mathrm{Pa} \cdot s$)	9.6×10^{-4}
Diffusion coefficient ($\frac{\mathrm{m}}{\mathrm{s}^2}$)	0.001
Initial pressure (Pa)	10^7
Initial saturation (-)	0.1
Left boundary condition: water injection rate ($\frac{\mathrm{m}^3}{\mathrm{day}}$)	0.2
Right boundary condition for pressure (Pa)	10^7
Left boundary condition for saturation (-)	0.9
Right boundary condition for saturation (-)	no change through the boundary

Table 2 Reservoir description: relative permeability curves (Corey model)

Endpoint relative permeability, oil	1
Endpoint relative permeability, water	1
Residual oil saturation	0.1
Connate water saturation	0.1
Corey exponent, oil	2
Corey exponent, water	2

Table 3 Reservoir description: measurement and model errors statistics

	Mean	Standard deviation
Pressure model errors ($\frac{1}{\mathrm{s}}$)	0	0.5×10^{-4}
Saturation model errors (-)	0	0.002
Pressure measurement errors (Pa)	0	10^5

References

1. Aziz, K., Settari, A.: Petroleum Reservoir Simulation. Applied Science Publishers LTD, London (1979)
2. Bennett, A.F.: Inverse Methods in Physical Oceanography. Cambridge University Press, New York (1992)
3. Bennett, A.F.: Inverse Modelling of the Ocean and Atmosphere. Cambridge University Press, Cambridge (2002)
4. Bennett, A.F., Muccino, J.C.: Generalized inversion of the Kortweg-de Vries Equation. Dyn. Atmos. Ocean. **35**, 227–263 (2002)
5. Chavent, G.M., DuPuy, M., Lemonnier, P.: History matching by use of optimal control theory. SPE J. **15**(1), 74–86 (1975)
6. Chen, W.H., Gavalas, G.R., Seinfeld, J.H., Wasserman, M.L.: A new algorithm for automatic history matching. SPE J. 593–608 (1974)
7. Courant, R., Hilbert, D.: Methods of Mathematical Physics. Interscience Publishers, Inc., New York (1966)
8. Jazwinski, A.H.: Stochastic Processes and Filtering Theory. Academic Press, New York (1970)
9. Li, R., Reynolds, A.C., Oliver, D.S.: History matching of three-phase flow production data. SPE J. **8**(4), 328–340 (2003)
10. Peaceman, D.W.: Fundamentals of Numerical Reservoir Simulation. Elsevier Scientific Publishing Company, Amsterdam (1977)
11. Przybysz-Jarnut, J.K.: Application of the Representer Method to Identify Uncertain Parameters in Large Scale Numerical Reservoir Models. MSc. thesis, Delft University of Technology, The Netherlands (2004)
12. Reid, L.B.: A Functional Inverse Approach for Three-Dimensional Characterization of Subsurface Contamination. PhD thesis, Massachusetts Institute of Technology, USA (1996)
13. Talagrand, O., Courtier, P.: Variational assimilation of meteorological observations with adjoint vorticity equation, I. Theory. Q.J.R. Meteorol. Soc. **113**, 1311–1328 (1987)
14. Valstar, J.R.: Inverse Modelling of Groundwater Flow and Transport. PhD thesis, Delft University of Technology, The Netherlands (2001)
15. Hanea, R.G., Heemink, A.W., Velders, G.J.M.: Data assimilation of ground level ozone in Europe with a Kalman filter and chemistry transport model. J. Geophys. Res. **109**, D 10302 (2004)